Proceedings of the 11th World Congress on Civil, Structural, and Environmental Engineering (CSEE 2026)
Paris, France - April, 2026
Paper No. ICSECT 145
DOI: 10.11159/icsect26.145

Numerical Analysis of Post-Tensioned Reinforced Concrete Beam-to-Column Joints

Erturk Tuncer[1], Can Karageyik[2], Erdem Canbay[2], Norgen Muka[2], Baris Binici[2]
[1]Department of Civil Engineering, TED University
Cankaya, Ankara 06420, Turkey
erturk.tuncer@tedu.edu.tr; can.karageyik@metu.edu.tr; ecanbay@metu.edu.tr; muka.norgen@metu.edu.tr; binici@metu.edu.tr
[2]Department of Civil Engineering, Middle East Technical University
Cankaya, Ankara 06800, Turkey

Abstract – Post-tensioning technology is particularly prominent for structures with long-span beams. The structural frame system is designed through an appropriate combination of prestressing and reinforcing steel, along with an optimal level of initial tendon stress. In this study, the effect of the mild steel amount on the seismic performance of post-tensioned cast-in-place reinforced concrete beams was investigated. Additionally, a conventional reinforced concrete beam was tested as a reference specimen to clarify the role of prestressing steel in the structural behavior. For this purpose, nonlinear finite element analyses were conducted to simulate the test beams, and a computer model was developed through calibration between the experimental results and numerical analyses. Subsequently, a parametric study was carried out to examine the variations in moment capacity and displacement ductility with respect to the top and bottom steel amounts. Lastly, a summary was prepared to compare the ultimate curvature, confined concrete strain, mild steel strain, and prestressing steel stress levels obtained from the tests, nonlinear analyses, and design requirements.

Keywords**:** Post-tensioning, cyclic loading, cast-in-place reinforced concrete, beam-to-column joint, finite element analysis

1. Introduction

Post-tensioning technology is widely applied in the floor systems of reinforced concrete (RC) buildings and various types of bridge structures. Additionally, it is utilized in the design of high-rise buildings, airports, silos, nuclear reactor vessels, and underground structures. In post-tensioned beams, mild steel is incorporated to resist a portion of the ultimate flexural moment. The non-prestressed reinforcement also mitigates excessive camber arising from the long-term creep of concrete, limits crack widths, and enhances ductility. Prestressing steel increases stiffness, improves self-centering capability, and reduces plastic deformations. Therefore, achieving an optimal balance between these two components is crucial for an efficient post-tensioned RC beam design. This concept, known as partial prestressing, aims to determine an appropriate arrangement of tendon and reinforcing steel to ensure a safe and economical structural performance. Kashiwazaki and Noguchi [1] examined the seismic performance of interior post-tensioned RC beam-to-column joints through experimental tests and nonlinear finite element (FE) analyses. They found that the prestressing force level had little effect on joint shear capacity, although higher prestressing levels led to smaller-angle cracking due to the self-centering action of the tendons. Hawileh et al. [2] performed three-dimensional nonlinear finite element analyses to evaluate the cyclic response of interior precast beam-to-column joints. The stress and strain distributions of both the mild reinforcement and post-tensioning tendons were examined. The results indicated that strand stresses remained below the yield level, while failure occurred due to the fracture of mild steel. A reasonable agreement was reported between the numerical predictions and experimental observations. Davey et al. [3] tested two half-scale exterior post-tensioned reinforced concrete beam-to-column connections designed in accordance with Australian requirements. One specimen had uniformly distributed strands, while the other featured tendons positioned closer to the joint region. Three-dimensional finite element analyses were also conducted to simulate the test setup. Experimental results showed that both specimens maintained their lateral load capacity up to a drift ratio of approximately 3%, and tendon layout had a negligible influence on overall behavior. The study further revealed that post-tensioning promoted crack closure during unloading, whereas higher prestressing levels reduced global ductility. Priestley and Tao [4] implemented an analytical study on the seismic performance of precast prestressed interior beam-

to-column joints with partially debonded tendons. They concluded that providing an appropriate debonding length on both sides of the column effectively reduced residual deformations. Paudel et al. [5] numerically examined the seismic response of post-tensioned precast wide U-shaped interior beam-to-column joints with different reinforcement configurations including spandrel reinforcement, prestressing strands, and A-truss rebars. Specimens comprising post-tensioning tendon and transverse reinforcement exhibited delayed crack initiation during cyclic loading. Moreover, combining prestressed and non-prestressed steel in the modified joints significantly enhanced the lateral load capacity relative to the control specimen. Zhipeng et al. [6] performed nonlinear finite element analyses to simulate contact surface behavior and plastic damage mechanisms in post-tensioned beam-to-column joints under cyclic loading. Zhou et al. [7] proposed a model considering residual deformation and energy dissipation to define damage indices for hybrid joints in self-centering frames. Fu et al. [8] developed numerical models of post-tensioned reinforced concrete beams with unbonded tendons to observe crack propagation and nonlinear strain distribution within damaged regions. Song et al. [9] introduced self-centering precast concrete frames utilizing hybrid joints to connect precast elements. They developed analytical models in OpenSees [10] and derived empirical equations to quantify the hysteretic energy demand distribution in hybrid joint-based self-centering structures. Morgen et al. [11,12] suggested a novel friction damper for unbonded post-tensioned precast concrete frame structures and developed a corresponding fiber–spring model. Analytical results demonstrated that friction-damped precast frames could achieve substantial energy dissipation while preserving strong self-centering capacity.

2. Laboratory Tests

Fig. 1 illustrates the prototype building floor plan and the test setup geometry. The steel reinforcement details and tendon configurations are also shown in Fig. 2. Accordingly, each specimen comprised columns with a cross section of 450 mm × 450 mm, beams measuring 400 mm × 400 mm, and a 100 mm-thick slab. The seismic design was executed in compliance with TBEC [13], whereas the post-tensioning design conformed to the provisions of ACI 318 [14]. In total, four specimens were tested. Among them, three specimens (S01, S02, and S03) were post-tensioned, with the amount of reinforcing steel serving as the main test variable. The other specimen (S04) was conventionally reinforced with mild steel only and used as a control. Table 1 provides a detailed summary of the material properties. In this table, $f_c^{'}$ and f_{pu} represent the compressive strength of concrete and the ultimate strength of tendon, respectively. Similarly, f_y and f_u denote the yield strength and ultimate strength of reinforcing steel. The post-tensioned beams were subjected to an effective prestress of approximately 1100 MPa, corresponding to nearly 60% of f_{pu}. Further details of experimental study might be found in the research performed by Karageyik et al. [15].

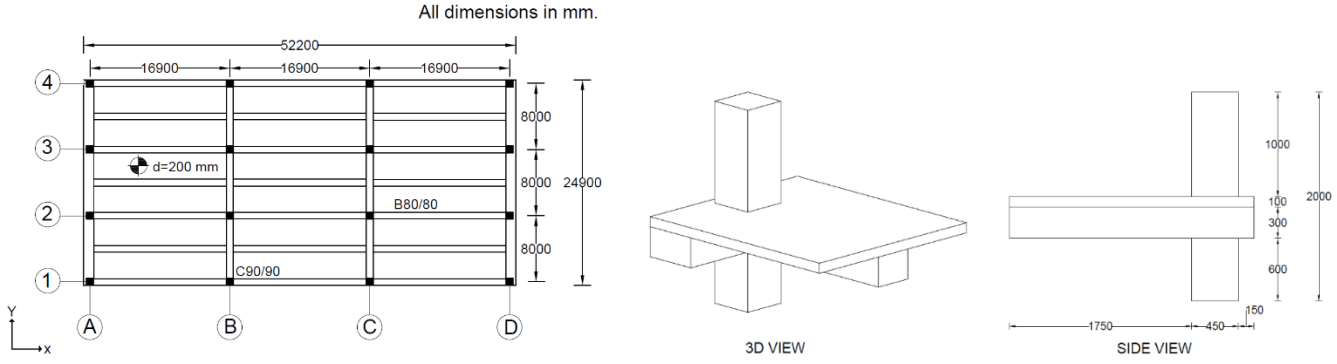

Fig. 1: Prototype building floor plan and test specimen geometry

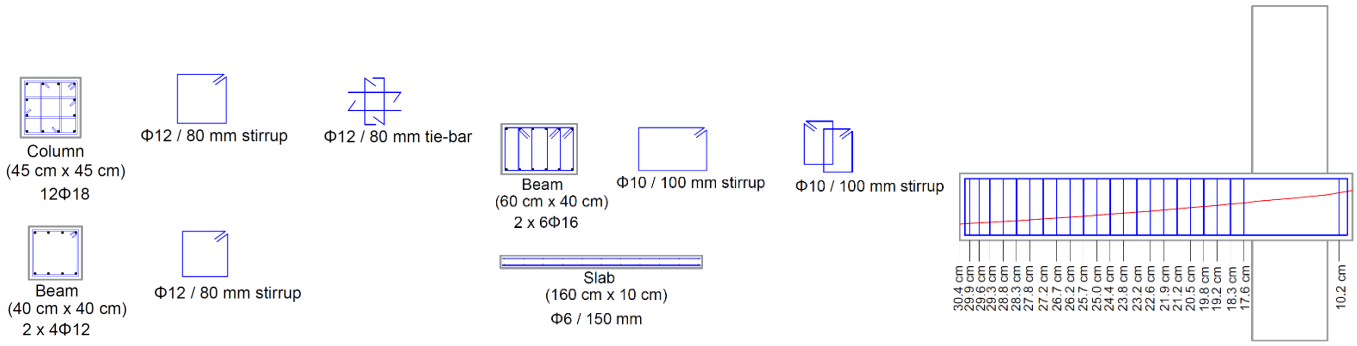

Fig. 2: Reinforcement details

Table 1: Properties of test specimens

Specimen	f_c' (MPa)	f_y (MPa)	f_u (MPa)	f_{pu} (MPa)	ρ,ρ'	A_{ps} (mm^2)
S01	44	557	692	1852	0.0030	2×150
S02	40	555	679	1849	0.0040	2×150
S03	46	553	645	1866	0.0067	2×150
S04	49	553	673	-	0.0100	-

(*)ρ: tension steel ratio, ρ': compression steel ratio, A_{ps}: tendon area.

3. Finite Element Simulations

Nonlinear finite element analyses were performed to simulate the structural responses of the specimens and make a comparison with the experimental findings [16]. The finite element model (FEM) was established based on the following assumptions:

(i) Concrete was modeled using four-node quadrilateral iso-parametric plane stress elements, referred to as Q8MEM.
(ii) One-dimensional embedded reinforcement elements were adopted for mild steel by assuming truss-like behavior.
(iii) Prestressing steel was modeled as reinforcement bars.

A parabolic stress–strain relationship was applied for unconfined concrete in compression (Fig. 3a), while the confined concrete regions enclosed by stirrups were modeled using the constitutive model proposed by Mander et al. [17]. The tensile behavior of concrete was represented by the model developed by Hordijk [18], as shown in Fig. 3b. The parameters of these constitutive relationships were derived from the study of Hendriks et al. [19]. The cyclic response of reinforcing steel, incorporating the Bauschinger [20] effect, followed the Menegotto–Pinto model [21] (Fig. 3c). Model parameters were selected based on the study of Deaton [22] and subsequently calibrated for specimen S03. The material properties summarized in Table 1 were employed to define the constitutive models.

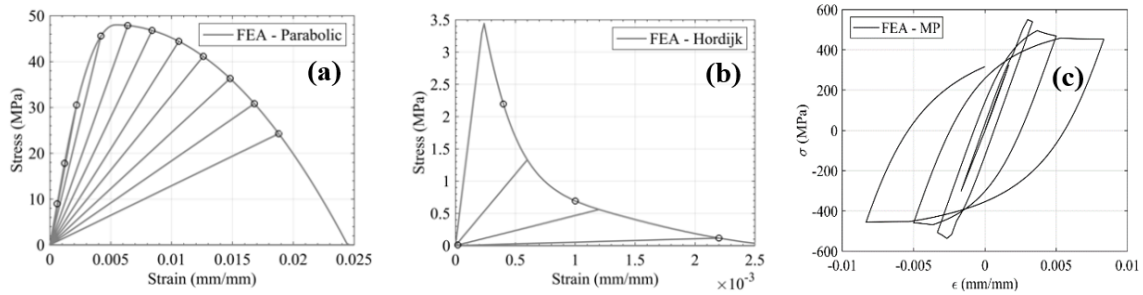

Fig. 3: Constitutive material models (a: concrete in compression, b: concrete in tension, c: reinforcing steel)

Fig. 4 indicates the comparison of base shear–lateral displacement relationships obtained from the finite element model and the experimental results. A reasonable agreement was achieved between the numerical simulations and the laboratory observations. The effects of mild steel amount on displacement ductility and moment capacity were also examined as introduced in Fig. 5 and Fig. 6, respectively. Based on these figures, while an increase in tension reinforcement was inversely correlated with displacement ductility, the inclusion of compression reinforcement improved the deformation capacity of the beam. Nevertheless, the contribution to the flexural strength was predominantly provided by the tension reinforcement, whereas the influence of compression reinforcement remained negligible.

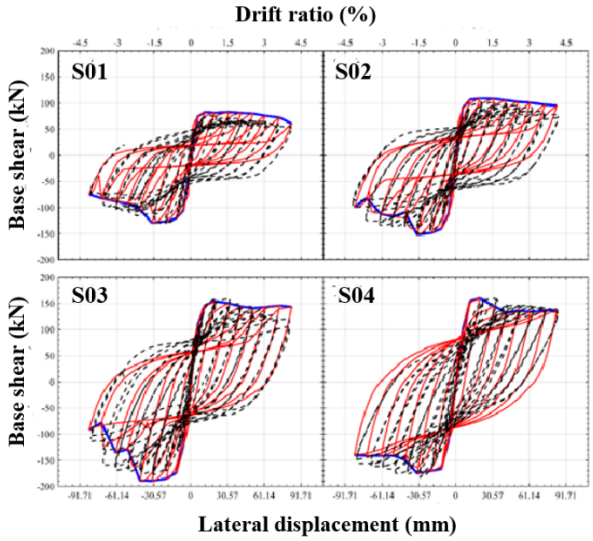

Fig. 4: Base shear-lateral displacement relationship

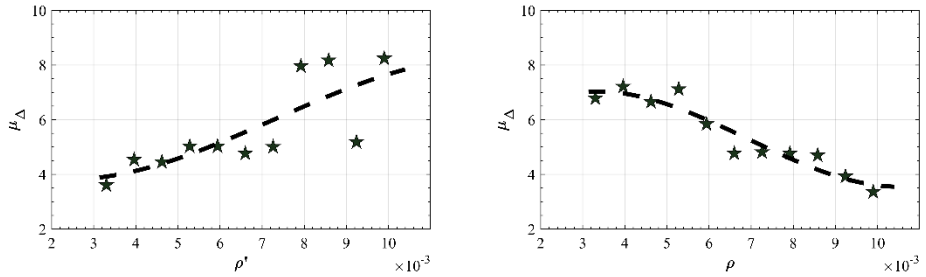

Fig. 5: Displacement ductility-mild steel ratio relationship

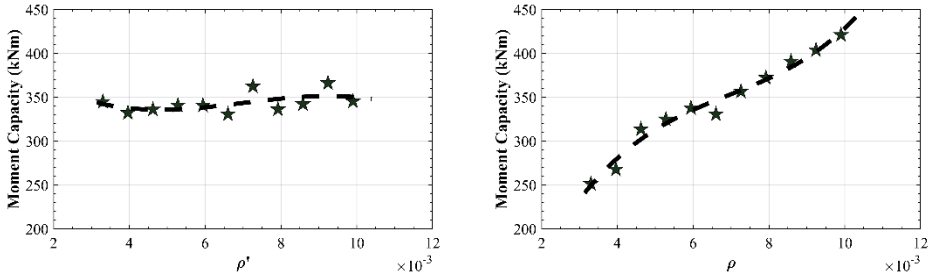

Fig. 6: Moment capacity-mild steel ratio relationship

The nonlinear finite element analyses were performed with three primary aims: (i) to examine the capability of the numerical model in capturing both local and global response characteristics—such as load–deflection trends and strain

distributions, (ii) to estimate the ductility capacity of post-tensioned reinforced concrete (RC) beams with different mild steel ratios based on experimentally calibrated models, and (iii) to evaluate the predicted ultimate curvature (ϕ_u), tendon stress (f_{ps}), and overall performance against experimental findings as well as the provisions of TBEC [13] and ACI 318 [14]. To achieve these objectives, strain data for both concrete and reinforcement within the plastic hinge regions were extracted from the analytical results, and corresponding curvatures were computed. According to TBEC [13], the ultimate confined concrete strain limit associated with the life safety (LS) performance level is expressed as ($\varepsilon_{cu} = 0.75\left(0.0035 + 0.04\sqrt{\frac{\alpha_{se}\rho_{sh}f_y}{f_c}} \leq 0.0135\right)$ where α_{se} is the confinement efficiency factor, ρ_{sh} is the transverse steel volumetric ratio). For the collapse prevention (CP) level, the code specifies a limiting steel strain of $\varepsilon_s = 0.4\varepsilon_{su}$, with ε_{su} being the strain corresponding to the maximum stress in the reinforcing steel. Fig. 7 presents the strain profiles derived from both finite element analyses and experimental observations, while Fig. 8 depicts the ultimate confined concrete strain values. Table 2 summarizes the comparisons of ultimate curvature, confined concrete strain, reinforcing steel strain, and tendon stress. Overall, the numerical predictions were in satisfactory agreement with the experimental data. The experimentally obtained ultimate curvature for the conventionally reinforced beam exceeded the analytical prediction by approximately 25%, whereas the maximum deviation among post-tensioned specimens was limited to about 10%. The ultimate confined concrete strains estimated by the finite element model corresponded to roughly 25–40% of the measured experimental values.

When the experimentally measured maximum confined concrete strains were evaluated against the TBEC [13] limits at a 3% interstory drift ratio, it was observed that the specimens were approaching the life safety boundary. In terms of reinforcing steel response, the discrepancy between the numerical and experimental ultimate strain values was approximately 25% for post-tensioned beams and around 60% for the specimen without post-tensioning. As indicated in Table 2, the ultimate reinforcing steel strains surpassed the collapse prevention threshold in all cases. Furthermore, the analytical results successfully replicated the tendon stress levels recorded during testing at a 3% drift ratio. Nevertheless, the tendon stress predicted by ACI 318 [14] was slightly higher than both experimental and analytical values, reflecting the inherent conservatism of the design recommendations. Further details of numerical study might be found in the research performed by Karageyik et al. [15].

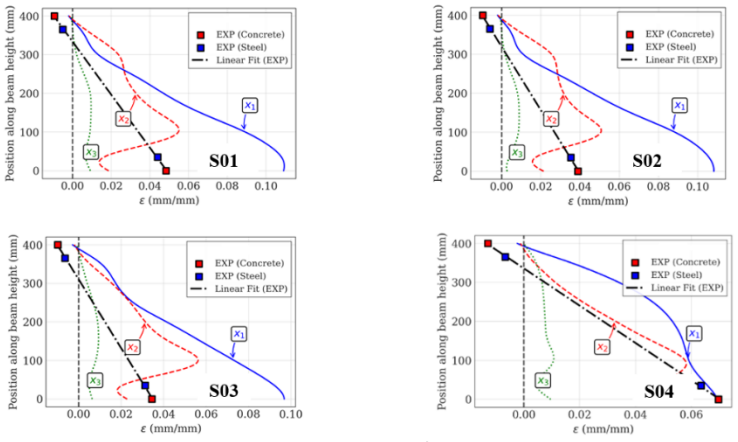

Fig. 7: Strain profile (*)

(*) Blue and red squares represent the experimentally measured strains of mild steel and concrete at the top and bottom levels, respectively. Strain distributions obtained from the finite element analyses were generated for various locations measured from the outer face of the column (i.e., $x_1 = 10$mm, $x_2 = 100$ mm, and $x_3 = 190$ mm).

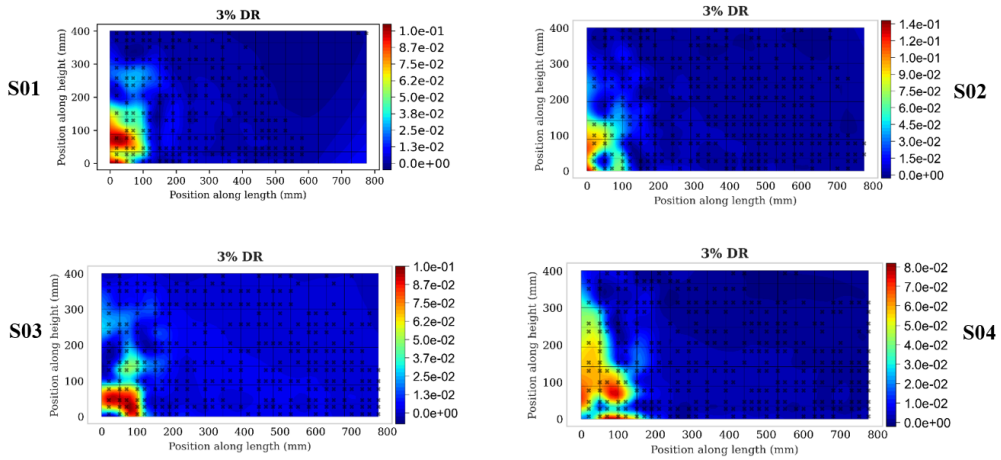

Fig. 8: Ultimate confined concrete strain

Table 2: Evaluation of key parameters based on test measurements, finite element analyses, and design codes

Parameter	S01			S02			S03			S04		
ϕ_u (rad/km)	Test	FEM		Test	FEM		Test	FEM		Test	FEM	
	144.0	139.6		121.4	134.8		111.2	125.1		206.7	166.4	
ε_{cu} (mm/mm)	Test	FEM	TBEC	Test	FEM	TBEC	Test	FEM	TBEC	Test	FEM	TBEC
	0.0093	0.0024	0.0101	0.0096	0.0029	0.0105	0.0098	0.0038	0.0099	0.0129	0.0032	0.0098
ε_s (mm/mm)	Test	FEM	TBEC	Test	FEM	TBEC	Test	FEM	TBEC	Test	FEM	TBEC
	0.044	0.044	0.032	0.035	0.042	0.032	0.031	0.039	0.032	0.064	0.040	0.032
f_{ps} at DR: 3% (MPa)	Test	FEM	ACI	Test	FEM	ACI	Test	FEM	ACI	Test	FEM	ACI
	1512	1347	1533	1164	1339	1515	1283	1492	1542	-	-	-

4. Conclusion

In this study, three post-tensioned reinforced concrete (RC) beams with varying mild steel ratios were examined through experimental testing and numerical modeling. The following conclusions were drawn from the results of this limited test program:

- The deformation capability of post-tensioned RC beams can be improved by providing an appropriate amount of mild steel reinforcement. As a result, a sufficiently ductile response is ensured under seismic loading scenarios.
- Nonlinear finite element analyses demonstrated the global load–deformation behavior of the test specimens with satisfactory accuracy. The predictions of tendon ultimate stresses and ultimate curvatures were consistent with the experimental observations. However, the accuracy in estimating local parameters, such as strains and crack widths, was lower, reflecting the inherent limitations of the smeared crack modeling approach.

Overall, post-tensioned beams can be effectively implemented in seismic regions when the mild steel reinforcement and tendon area are appropriately proportioned. On the other hand, further research involving detailed nonlinear time-history analyses is recommended to refine the response modification factors and enhance design guidelines for post-tensioned RC members.

Acknowledgements

The authors would like to thank the Scientific and Technological Research Council of Turkey (TUBITAK). This work was supported by the Scientific and Technological Research Council of Turkey (TUBITAK) under grant number 119M973.

References

[1] T. Kashiwazaki, H. Noguchi, "Seismic performance evaluation of beam-column joints for prestressed RC buildings with high performance materials," *High Performance Materials in Bridges*, 406–415. https://doi.org/https://doi.org/10.1061/40691(2003)36, 2001.

[2] R. A. Hawileh, A. Rahman, H. Tabatabai, "Nonlinear finite element analysis and modeling of a precast hybrid beam-column connection subjected to cyclic loads," *Applied Mathematical Modelling*, *34*(9). https://doi.org/10.1016/j.apm.2009.11.020, 2010.

[3] M. J. Davey, K. Abdouka, R. Al-Mahaidi, "Exterior post-tensioned band beam to column connections under earthquake loading," *Australian Journal of Structural Engineering*, *17*(1). https://doi.org/10.1080/13287982.2015.1116179, 2016.

[4] M. J. N. Priestley, J. R. Tao, "Seismic response of precast prestressed concrete frames with partially debonded tendons," *PCI Journal*, *38*(1). https://doi.org/10.15554/pcij.01011993.58.69, 1993.

[5] S. Paudel, G. Tanapornraweekit, S. Tangtermsirikul, "Numerical study on seismic performance improvement of composite wide beam-column interior joints," *Journal of Building Engineering*, *46*. https://doi.org/10.1016/j.jobe.2021.103637, 2022.

[6] G. Zhipeng, G. Haishan, L. Liming, S. Pengfei, L. Siyao, Z. Yunfeng, Z. Jian, "Nonlinear finite element analysis of post tensioned precast prestressed slab-beam-column joints," *Structures*, *58*. https://doi.org/10.1016/j.istruc.2023.105438, 2023.

[7] Y. Zhou, G. Song, W. Huang, "Performance-based damage evaluation of hybrid joints," *Bulletin of Earthquake Engineering*, *18*(8), 3781–3816. https://doi.org/10.1007/s10518-020-00838-8, 2020.

[8] C. Fu, Y. Zhu, Y. Wang, "Stiffness assessment of cracked post-tensioned concrete beams with unbonded tendons based on the cracking pattern," *Engineering Structures*, 214, https://doi.org/10.1016/j.engstruct.2020.110599, 2020.

[9] L. L. Song, T. Guo, C. Chen, "Experimental and numerical study of a self-centering prestressed concrete moment resisting frame connection with bolted web friction devices," *Earthquake Engineering and Structural Dynamics*, *43*(4). https://doi.org/10.1002/eqe.2358, 2014.

[10] F. McKenna, "OpenSees: A framework for earthquake engineering simulation," *Computing in Science and Engineering*, *13*(4). https://doi.org/10.1109/MCSE.2011.66, 2011.

[11] B. G. Morgen, Y. C. Kurama, "A friction damper for post-tensioned precast concrete moment frames," *PCI J.* 49(4). https://doi.org/10.15554/pcij.07012004.112.133, 2004.

[12] B. G. Morgen, Y. C. Kurama, "Seismic response evaluation of posttensioned precast concrete frames with friction dampers," *Journal of Structural Engineering*, *134(1)* https://doi.org/10.1061/(ASCE)0733-9445(2008)134:1(132), 2008.

[13] Turkish Standards. *Turkey building earthquake code* (TBEC), 2018.

[14] American Concrete Institute. *Building code requirements for structural concrete* (ACI 318), 2019.

[15] C. Karageyik, E. Tuncer, B. Binici, E. Canbay, N. Muka, "Seismic response of post-tensioned reinforced concrete beams," *Structures*, *75.* https://doi.org/10.1016/j.istruc.2025.108841, 2025.

[16] Diana, "User's Manual - Release 9.4.4," *TU Delft: TNO Building and Construction Research*, 2012.

[17] J. B. Mander, M. J. N. Priestley, R. Park, "Theoretical stress-strain model for confined concrete," *Journal of Structural Engineering*, *114*(8), 1804–1826. https://doi.org/10.1061/(asce)0733-9445(1988)114:8(1804), 1988.

[18] D. A. Hordijk, "Local approach to fatigue of concrete*," Doctoral dissertation*, Delft University of Technology, 1991.

[19] M. A. N. Hendriks, A. Boer, B. Belletti, "Guidelines for Nonlinear Finite Element Analysis of Concrete Structures*," Rijkswaterstaat Centre for Infrastructure*, Report RTD:1016-1, 2017.

[20] J. Bauschinger, "On the change of the position of elastic limit of iron and steel under cyclic variation of stress*," Mitt. Mech.-Tech. Lab,* Munich, 13 (1), 1886.

[21] M. Menegotto, P. E. Pinto, "Method of analysis of cyclically loaded RC plane frames including changes in geometry and non-elastic behavior of elements under normal force and bending," *Preliminary Report IABSE*, vol 13,1973.
[22] J. B. Deaton, "Nonlinear finite element analysis of reinforced concrete exterior beam-to-column joints with nonseismic detailing," *Doctoral dissertation*, Georgia Institute of Technology, 2013.